Pass-band Balanced Steady State Free Precession Functional MRI of the Mouse Retina

E. R. Muir[1,2], S-H. Park[3], and T. Q. Duong[2]

[1]Biomedical Engineering, Georgia Institute of Technology, Atlanta, GA, United States, [2]Research Imaging Institute, Ophthalmology/Radiology, UT Health Science Center San Antonio, San Antonio, TX, United States, [3]Research Imaging Institute, Radiology, UT Health Science Center San Antonio, San Antonio, TX, United States

Introduction: The retina (~270 µm thick) is nourished by two distinct vascular layers, the retinal and choroidal circulations. The photoreceptors, located roughly in the middle of the retina in between the two vascular layers, are avascular (1). High-resolution BOLD fMRI of the retina (90x90 µm) to different physiological stimulations has been reported using echo-planar imaging (EPI) (1). While EPI offers rapid acquisition, it is more susceptible to artifacts, such as geometric distortion, signal dropout, and spatial resolution degradation due to long readout time in the phase-encoding direction. EPI of the retina is particularly susceptible because the eye is located in a region of large magnetic inhomogeneity and very high-resolution is needed, pushing gradient limits with EPI (i.e., high bandwidth readout, large gradient magnitude and slew rate). In this study, we implemented pass-band balanced steady state free precession (bSSFP) fMRI (2,3) in the mouse retina to overcome the mentioned limitations of EPI while maintaining rapid acquisition capability and high SNR per unit time. We further demonstrated that bSSFP fMRI could reliably detect layer-specific responses to hypoxic challenge at 45x45x500 µm.

Methods: Male C57BL/6 mice (6-10 weeks, n=6) were imaged under 1.1% isoflurane and spontaneous breathing. Respiration rate, heart rate, oxygen saturation, and temperature were monitored and maintained. Hypoxic challenge involved 4.5 min baseline (30% O_2 in N_2) and 4.5 min of hypoxia (10% O_2 in N_2). MRI was done on a 7T/30cm Bruker scanner with 100 G/cm gradient using a surface eye coil (ID = 0.6 cm). Images were acquired in coronal orientation using bSSFP with a 5x5 mm FOV, 112x112 matrix (45x45 µm), one 0.5 mm thick slice, and 3.67/7.34 ms TE/TR. FASTMAP shimming was used to reduce banding and the RF phase cycling was adjusted to move bands away from the retina. Automated profile analysis (1) was performed to align the retina and calculate %-changes along the length of the retina.

Results: As **Figure 1** shows, EPI of the retina has severe distortions. Depending on the direction of phase-encoding acquisition, the distortion yielded either compression or stretching of the image. In contrast, bSSFP produced images without distortion. Four distinguishable dark-bright-dark-bright retinal layers were detected in the bSSFP image with uniform structure along the retina. One to three distinguishable retinal layers were usually detected in EPI with non-uniform structure and thickness along the retina. **Figure 2A** shows a representative %-change map associated with hypoxic challenge from a single mouse using bSSFP. Hypoxia decreased the signal in the retina, with a stronger response in the choroid vascular layer than the retinal vascular layer. Anatomy profiles during baseline and hypoxia (**Figure 2B**) show four alternating dark-bright-dark-bright layers. **Figure 2C** shows the corresponding %-change profile due to hypoxia. Two well resolved layers were detected that showed signal reductions. These layers were assigned to be the retinal and the choroidal vascular layer. The middle layer in between these two vascular layers showed no significant change and was assigned as the avascular photoreceptor layer. The group-averaged %-changes were -12.3±2.09% in the inner (retinal) layer ($p<5E-4$ control vs. baseline), -1.86±2.06% in the middle (photoreceptor) layer ($p=0.06$), and -29.7±3.42% in the outer (choroid) layer ($p<5E-7$) (mean±SD, n= 6). The %-changes in the middle layer were statistically different from that of the inner ($p<5E-4$) and outer layer ($p<5E-6$). The %-change of the inner and outer layer were also statistically different ($p<5E-4$).

Discussion: This study demonstrates for the first time high spatial resolution pass-band bSSFP fMRI of the retina without susceptibility-induced signal drop out and image distortion. The temporal resolution and SNR per unit time are comparable to EPI. It has been reported that pass-band bSSFP fMRI yields contrast similar to T_2 or T_2* BOLD (3), but the sources of the bSSFP fMRI signals have been unclear, with dependence on TR/TE and field strength. Further study is necessary to understand the signal sources under our scan conditions. Nonetheless, the bSSFP parameters that were used showed sensitivity to oxygenation changes.

The signal decrease due to hypoxia was larger in the choroid than retinal vessels, likely a result of high basal choroid blood volume and blood flow (4). This finding is consistent with a previous MRI study using EPI which demonstrated layer-specific BOLD responses to hyperoxia and hypercapnia in the rat retina at lower resolutions, 90x90x1000 µm (1). By comparison, we report layer-specific bSSFP fMRI at much higher resolution and with clearer separation than previously reported.

Four anatomical layers were clear in the bSSFP images. The %-change peak of the choroid lined up with the outermost bright layer of the anatomy. The %-change peak of the retinal layer appears to span the inner dark and bright layer of the anatomy. The dark layer in the middle of the retina is therefore likely the photoreceptors, although further experiments are needed to assign these anatomical layers.

Conclusion: Pass-band bSSFP fMRI of the retina yields high spatial and temporal resolution without geometric distortion and signal dropout. This approach detects separate responses of the retinal and choroidal vasculature. The bSSFP fMRI approach has comparable temporal resolution and SNR per unit time as EPI BOLD fMRI but without the susceptibility artifacts associated with EPI. Future studies will expand to include visual stimulations, blood flow contrast, and applications to retinal diseases.

Reference: 1) Cheng et al, PNAS 2006, 103:17525. 2) Zhong et al, MRM 2007, 57:67. 3) Miller & Jezzard, MRM 2008, 60:661. 4) Alm & Bill, Exp Eye Res 1973, 15:15. Funded by R01 EY014211, R01 EY018855, VA MERIT.

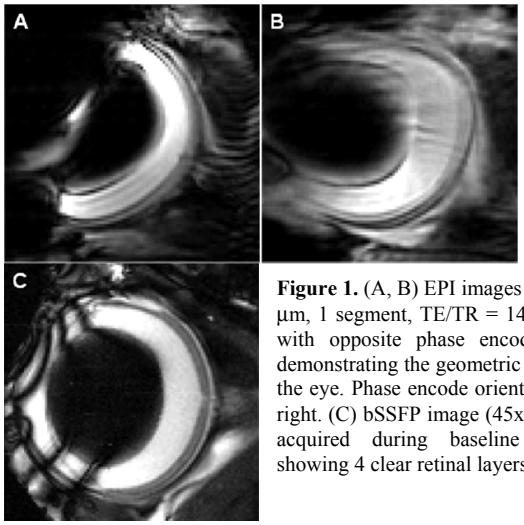

Figure 1. (A, B) EPI images (47x47x600 µm, 1 segment, TE/TR = 14.9/3000 ms) with opposite phase encoding orders, demonstrating the geometric distortion in the eye. Phase encode orientation is left-right. (C) bSSFP image (45x45x500 µm) acquired during baseline conditions showing 4 clear retinal layers.

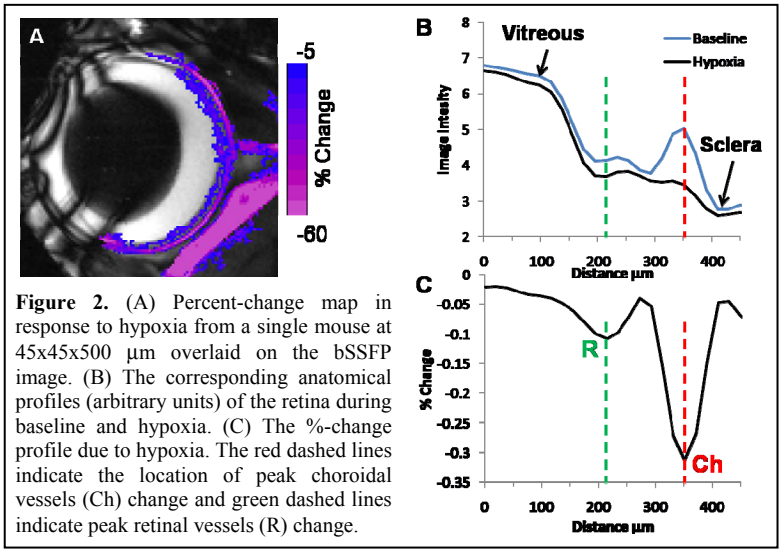

Figure 2. (A) Percent-change map in response to hypoxia from a single mouse at 45x45x500 µm overlaid on the bSSFP image. (B) The corresponding anatomical profiles (arbitrary units) of the retina during baseline and hypoxia. (C) The %-change profile due to hypoxia. The red dashed lines indicate the location of peak choroidal vessels (Ch) change and green dashed lines indicate peak retinal vessels (R) change.